ORIGINAL ARTICLE

Received: Mar 16, 2024

Revised: Dec 03, 2024

Approved: Dec 23, 2024

Evaluation of the interference of metallic dental artifacts with virtual implant planning

on CBCT

Marcos Antônio Lima dos Santos¹, Aline Piruna Martins Santos¹, Wilton Mitsunari

Takeshita², Giuseppe Alexandre Romito¹, Lucas Alves da Mota Santana³, Vítor Marques

Sapata⁴, Marcelo Gusmão Paraíso Cavalcanti¹

¹Departamento de Estomatologia, Faculdade de Odontologia, Universidade de São Paulo

(USP) – São Paulo (SP), Brazil

²Departamento de Diagnóstico e Cirurgia, Faculdade de Odontologia, Universidade Estadual

Paulista (Unesp) – Araçatuba (SP), Brazil

³Departamento de Odontologia, Universidade Federal de Sergipe (UFS) – Aracaju (SE),

Brazil

⁴Departamento de Odontologia, UniCesumar – Maringá (PR), Brazil

Corresponding author: Marcos Antônio Lima dos Santos - Departamento de Estomatologia,

Faculdade de Odontologia, Universidade de São Paulo - Avenida Prof. Lineu Prestes, 2227 -

Cidade Universitária – CEP: 05508-000 - São Paulo (SP), Brazil - E-mail:

marcosals@outlook.com.br

Declaration of interest: nothing to declare

Financial support: CAPES (Finance Code 001)

© The authors

1

ABSTRACT

Introduction: The quality of cone-beam computed tomography (CBCT) images can be

affected by patient factors, including metal artifacts, which may compromise diagnosis and

surgical planning. Objective: To evaluate the interference of metal restoration artifacts with

superimposed DICOM and STL files using automatic segmentation in CBCT planning software

and compare it with image acquisition. Methods: Subjects were divided into three groups:

group 0 (zero to two restorations), group 1 (three to five restorations), and group 2 (six or more

restorations). DICOM files were superimposed on STL files using four fixed anatomical

positions in 3D arches for standardization. Statistical analysis included Shapiro-Wilk normality,

Levene, Kruskal-Wallis, Dunn's post-tests, and Mann-Whitney U Test, with a 5% significance

level. **Results:** The mean deviation was 0.489 mm (SD $\pm 1.353 \text{ mm}$). The number of restorations

significantly influenced deviations in the horizontal/anterior position (p=0.009). Group 1

differed significantly from group 2, while group 0 showed no significant differences from

either. Comparing occlusion and non-occlusion, Vertical/Posterior (VP) and Vertical/Anterior

(VA) positions showed significant differences, with higher means for group 1. Conclusion:

Metal artifacts did not affect vertical analyses in CBCT planning but caused discrepancies in

horizontal DICOM-STL segmentation adjustments.

Keywords: Dental Implants; Artifacts; Computer-Aided Design; Image Processing, Computer-

Assisted; Cone-Beam Computed Tomography.

2

INTRODUCTION

Implant-guided surgery involves placing dental implants using surgical guides produced by CAD-CAM technology. Planning software designs the surgical guide on tooth surface models with stereolithography (STL) files, which are superimposed and recorded on tomographic files (DICOM). Thus, planning can occur in a virtual environment where soft and hard tissue information is connected and aligned in the same setting, helping identify anatomical deviations. That may affect surgery and implant placement regarding the best three-dimensional position for future prosthetic rehabilitations. After planning, the guide is designed and exported for further fabrication using 3D printers. However, the quality of STL and DICOM file acquisition may harm this technique^{1,2}.

Patient factors, movement during the exam, voxel size, contrast resolution, and artifacts of different sources may impair cone-beam computed tomography (CBCT) image quality^{3,4}. An imaging artifact is a structure visualized alongside the image formed with the reconstruction data but not present on the object from which the image was acquired⁵. Artifacts may impair diagnosis and surgical planning, affecting the visualization of different structures or even bone defects, such as peri-implant bone, fenestrations, and furcation lesions^{6,7}.

Correct image registration requires capturing multiplanar reconstructions in a high image resolution, considering that any changes can cause model inaccuracies^{8,9}. Moreover, dental restorations may increase the imprecision level due to artifact formation, causing image registration errors in CBCT images¹⁰⁻¹².

The null hypothesis was that artifacts from metallic dental restorations do not affect image registration failures between DICOM and STL files with automatic segmentation using CBCT planning software, comparing this interference with the acquisition of images in occlusion and non-occlusion.

Therefore, this study aimed to evaluate the interference of artifacts from metallic dental restorations with superimposed images, with automatic segmentation using CBCT planning software, and compare this interference with image acquisition in occlusion and non-occlusion.

METHODS

Patient selection and group assignment

The imaging acquisitions were approved by the Research Ethics Committee registered with the CAAE: 82950618.2.0000.0075 and Opinion number: 2,523,002.

This study is a retrospective study that used CT scan files in DICOM format acquired from a ProMax 3D Max cone-beam computed tomography unit (Planmeca, Helsinki, Finland), using the following protocol: 90 kVp, 12 mA, FOV 13x9 cm, and 0.16 mm voxel. A trained dentist also performed intraoral scans (Virtuo Vivo 3.4, Dental Wings, Canada). The scanning was performed in a standardized way, starting with the palatal/lingual surface, followed by the occlusal surface, and ending with the buccal surface. In a second moment, the gaps in the initial scan were randomly filled by the operator through focal scanning of areas not previously captured. Through smooth and linear movement, the operator kept the scanner at a distance of approximately 5mm from the faces to be scanned. The scanner used has an accuracy of about 40 µm according to the manufacturer.

The database provided 100 tomographic exams, designated through sample calculation, of which 97 were selected for evaluation according to the following inclusion criteria: 1) Partially edentulous patients with restorations or fixed metal prostheses; 2) Patients with dental implants; 3) Patients with at least one anterior and one posterior tooth. The exclusion criteria were as follows: 1) Patients with metal restorations on all teeth; 2) Patients only with dental implants; 3) Fully edentulous patients.

Image data import and segmentation

Tomographic data in DICOM format and intraoral scanning in STL format (stereolithography) were imported into Blue Sky Plan software (Version 4.9.4, Libertyville, IL, USA). Two oral and maxillofacial radiologists experienced in using implant planning software, blinded to patient clinical data and did not participate in the intraoral scans, segmented the CBCT data. Subsequently, the metal restorations in CBCT images were counted with the overlaid STL files using the automatic tool of the software before the experimental phase. Software instructions were provided. The "screenshot" tool was used to illustrate the coronal and sagittal images segmentation that were saved and measured with the CBCT data available in DICOM format and intraoral scanning (Figure 1).

As for the qualitative image evaluation, clippings were made from the software in sagittal and coronal images to verify a potential image registration error between the STL and DICOM systems (Figure 2).

Image registration protocol

The DICOM files were selected and superimposed on their corresponding STL file based on four fixed anatomical positions in the 3D arches, as identical as possible, to standardize the superposition. These milestones were defined as described below and indicated in Figure 1: A) Vertical/Posterior (VP): Selecting a posterior tooth and measuring the distance between the STL file and the occlusal surface of the tooth (cuspid tip). B) Horizontal/Posterior (HP): After selecting a posterior tooth, the distance between the STL file and the buccal surface was measured. C) Vertical/Anterior (VA): Selecting an anterior tooth and measuring the distance between the STL file and the incisal surface of the tooth. D) Horizontal/Anterior (HA): After selecting an anterior tooth, the distance between the STL file and the buccal surface was measured.

The subjects were divided into three groups to analyze the artifact/restoration: group 0 included patients with zero restorations, group 1 had patients with three to five restorations, and group 2 consisted of patients with six restorations or more. The number of individuals per group varied according to the position analyzed. Each patient was assessed for one anterior and one posterior element. Each element was subjected to standardized measurements vertically to the STL file in the incisal or occlusal surface and horizontally to the STL file in the cervical third of the face. The same procedure analyzes the images of patients in these same positions, but patients in occlusion would be allocated to group 0 and those in non-occlusion to group 1. There were two groups for arch type according to the occlusion pattern, in which group 0 was selected for the maxilla and group 1 for the mandible.

Data record evaluation

The scan image registration accuracy in the DICOM file was evaluated by measuring the distance between the scan and the 3D volume using the visualization software, ImageJ (National Institutes of Health, USA, Maryland). Reference points were selected for the measurements: one on the incisal surface for anterior teeth, one on the cusp tip for posterior teeth, and one on the buccal surface coinciding or close to the cementoenamel junction (CEJ) for both positions. Thus, four distances were recorded for each model. When this reference point was not visible or missing due to the absence of a dental element, the most distal occlusal and incisal surfaces were used. If none of these regions could be visualized, the measurement was omitted. Two distances were recorded for each dental element: one toward the long axis of the tooth from the incisal surface of anterior teeth or the cusp tip of posterior teeth, and one perpendicular to the buccal surface up to the STL tracing.

Statistical analysis

To evaluate intra-examiner and inter-examiner agreement, the intraclass correlation coefficient (ICC) was applied. The data were statistically analyzed with the Shapiro-Wilk normality and Levene tests to assess homoscedasticity. Kruskal-Wallis and Dunn's post-tests analyzed the artifacts, and the Mann-Whitney U Test investigated occlusion and arch type. This study used SPSS for Windows 20.5 (SPSS, Chicago, IL), BioEstat 5.0 (Instituto Mamirauá, Belém, PA), and GraphPad Prism (GraphPad Software, San Diego, CA). All tests used a 5% significance level.

RESULTS

The ICC values for examiner 1 were 0.98, and for examiner 2 were 0.96. The ICC value between evaluators was 0.93, indicating excellent replicability according to Fleiss. This study found a mean of 0.489 mm and a standard deviation of ± 1.353 mm. The analysis of variance showed a significant influence of the number of metal restorations on the deviations of models in the horizontal/anterior position (p=0.009), and Dunn's post-test was applied (Table 1).

According to the box plot in Figure 3, group 1 showed a statistically significant difference from group 2. Group 0 did not significantly differ from groups 1 and 2.

Boxplot showing median, maximum, and minimum, with the application of the Kruskal-Wallis test and post-Dunn's test. Different letters (AB) represent a statistically significant difference between groups (Figure 3).

Table 2 displays occlusion and non-occlusion comparisons, showing a statistically significant difference in VP and VA positions. In both cases, group 1 showed a higher meaning.

The occlusion during tomographic acquisition shows that the VP (p=0.029) and VA (p=0.006) positions showed statistically significant differences.

Table 3 refers to upper and lower arches according to the occlusion pattern, showing a statistically significant difference in VP and VA positions. In both cases, group 1 showed a higher meaning.

DISCUSSION

The null hypothesis was rejected due to statistically significant differences between the groups according to occlusion type and the number of metal restorations. Metal objects in the field of view (FOV) can produce artifacts from three sources: scattering, beam hardening, and starvation. However, the higher the values of these three sources, the higher the attenuation of X-ray photons. Consequently, the signal collected by the receiver will drastically decrease 13,14.

CBCT cannot provide accurate intercuspation and occlusal surface due to poor scanning resolution and streak artifacts from metal restorations, insufficient exposure of the teeth, and complicating a full surgical guide settling at placement surgery¹⁵⁻¹⁷. Therefore, integrating a virtual impression of teeth and related oral structures from an intra- or extraoral surface requires a complementary scan with an accurate anatomical morphology of the dentition and its interocclusal relationship¹⁸.

In our sample, it was not always possible to perform the procedure in occlusion, since some patients did not have most of their anterior teeth, preventing them from keeping their vertical dimension correctly positioned, considering that the stability maintained by these teeth was not achieved. In our study, mostly partial volume artifacts were found, mainly in the presence of orthodontic brackets and crowns, generating shadows or striations, which, in turn, despite slightly distorting the image quality, were not sufficient to prevent the superimposition of the DICOM-STL system in most cases.

Metals produced streak artifacts in DICOM files, and, considering that patients present metal restorations, finding reliable reference points for recording positions becomes

challenging¹⁹. Studies indicated procedures to reduce the beam hardening effect of artifacts, such as the Metal Artifact Reduction (MAR) tool, which minimizes gray value variability and increases the contrast-to-noise ratio, highly increasing image quality and ease of image registration systems^{20,21}.

Some articles demonstrated deviations between the planned implant and its actual position, with a reported mean of 1.12 mm, and such deviations cause cumulative errors throughout the guided implant planning protocol^{22,23}. Considering this gap in the literature regarding studies on the influence of deviation data recording, especially in the presence of metal restorations, because there was no consensus on the best method, our study was developed to elucidate this relationship between the presence of metal artifacts and image registration failures.

This study proposed to verify whether the number of metal restorations interferes with the automatic superimposition of STL and DICOM files and analyze the potential implications for open- or closed-mouth acquisitions. The results were relevant since the analysis of variance showed statistically significant data on model deviations in different demarcated positions, determining the image registration accuracy corresponding to imaging artifacts and showing the potential interference of metal artifacts with planning modalities.

The literature review showed three systems documented for collecting and analyzing patient data, allowing, by different procedures, the superposition of hard and soft tissues for prosthetic planning, which are DICOM-DICOM, DICOM-cast, and DICOM-STL²⁴⁻²⁶. The present study used the DICOM-STL protocol, which is based on the superposition of DICOM data from CBCT and STL data from a scan (intra- or extraoral). Common landmarks understood as visible areas in both files were used for image registration of the two datasets²⁷.

CBCT allows for visualizing hard tissue, and intra- and extraoral scanning gathers information about the soft tissues of these patients. Thus, superimposed DICOM files with STL create a "virtual patient" and can be used in implant planning procedures^{28,29}.

Artifacts from metal³⁰ materials can cause image registration failure in automatic planning systems due to beam hardening, resulting in altered images, forming hypodense bands (dark bands), hyperdense striations (white streaks), and distorting metal objects (cupping artifacts). The present study analyzed the comparative data on the number of metal restorations in the four positions, obtaining only a statistically significant difference in the horizontal/anterior position (p=0.009), corroborating a previous study³¹ that stated that the anterior region produced more artifacts than the posterior one. Figure 2 shows software effectiveness in all conditions, except for the HA group, which has few artifacts, indicating satisfactory accuracy with considerably fewer metal artifacts or a high number of them because the number of metal artifacts in CBCT images can significantly affect image quality, corroborating different authors^{32,33}. That might indicate two situations: the first would infer that a high number of artifacts hindered the analysis in the visualization software, and the second would refer to software ineffectiveness in the presence of few metal artifacts^{34,36}.

The present work also evaluated the difference between these artifacts in the dental arches, corresponding to the maxilla and mandible in their respective positions. There were statistically significant differences in both VP and VA positions, and the mandible showed the highest number of artifacts compared to the maxilla. These results corroborated with some studies^{5,32}, requiring more caution when evaluating this area in an overlapping plan.

It is worth noting that, in the horizontal analysis, the artifacts in the upper and lower arches did not interfere with the posterior and anterior bites of patients. The vertical analysis in both positions showed statistically significant values, demonstrating the interference of these metal artifacts with image registration in this evaluation. The horizontal variation showed little

interference whether the patient was in occlusion or not because there were few metal artifacts, and the face was free. The vertical positions with occlusion demonstrated a loss of references that define the verticality of STL files, causing anterior and posterior discrepancies.

Moreover, the results were statistically significant in the vertical posterior and vertical anterior positions, where the relationship between the distance from STL to its dental occlusion positions (occlusal/incisal) was analyzed. That may help understand that metal artifacts interfere with the correct software measurement when registering these images, resulting in unfeasible planning.

The research presented limitations regarding metal restorations, considering that each metal material has a different atomic number and, consequently, affects the expression of artifacts and gray values in CBCT, as stated in several works³²⁻³⁶. Protocols that decrease artifact production in CBCT should be included when planning with overlaid images because they interfere with the reliable reproduction of planning models in guided surgeries. Further studies should be performed to assess software effectiveness in the presence of artifacts from metal materials.

Conclusion

This study concluded that, whether the patient is in occlusion or not, metal artifacts do not interfere with CBCT planning software for superimposed images in vertical analyses. However, horizontally, there was an inferred discrepancy in the adjustments to DICOM-STL segmentation. Additionally, metal artifacts distorted the superimposition and hindered the planning of procedures using this technique. Protocols that reduce metal artifacts should be used to improve image quality without harming the image registration procedure.

REFERENCES

- 1. Flügge TV, Att W, Metzger MC, Nelson K. Precision of dental implant digitization using intraoral scanners. Int J Prosthodont. 2016;29(3):277-83. https://doi.org/10.11607/ijp.4417
- 2. Kamio T, Suzuki M, Asaumi R, Kawai T. DICOM segmentation and STL creation for 3D printing: a process and software package comparison for osseous anatomy. 3D Print Med. 2020;6(1):17.

https://doi.org/10.1186/s41205-020-00069-2

- 3. Jacobs R, Salmon B, Codari M, Hassan B, Bornstein MM. Cone beam computed tomography in implant dentistry: recommendations for clinical use. BMC Oral Health. 2018;18(1):88. https://doi.org/10.1186/s12903-018-0523-5
- 4. Oliveira MR, Sousa TO, Caetano AF, Paiva RR, Valladares-Neto J, Yamamoto-Silva FP, et al. Influence of CBCT metal artifact reduction on vertical radicular fracture detection. Imaging Sci Dent. 2021;51(1):55-62.

 $\underline{https://doi.org/10.5624/isd.20200191}$

- 5. Terrabuio BR, Carvalho CG, Peralta-Mamani M, Santos PSS, Rubira-Bullen IRF, Rubira CMF. Cone-beam computed tomography artifacts in the presence of dental implants and associated factors: an integrative review. Imaging Sci Dent. 2021;51(2):93-106. https://doi.org/10.5624/isd.20200320
- 6. Pinheiro LR, Gaia BF, Sales MAO, Umetsubo OS, Santos Junior O, Cavalcanti MG. Effect of field of view in the detection of chemically created peri-implant bone defects in bovine ribs using cone beam computed tomography: an in vitro study. Oral Surg Oral Med Oral Pathol Oral Radiol. 2015;120(1):69-77.

https://doi.org/10.1016/j.oooo.2015.04.006

7. Pinheiro LR, Scarfe WC, Augusto de Oliveira Sales M, Gaia BF, Cortes AR, Cavalcanti MG. Effect of Cone-Beam Computed Tomography Field of View and Acquisition Frame on the Detection of Chemically Simulated Peri-Implant Bone Loss In Vitro. J Periodontol. 2015;86(10):1159-65.

https://doi.org/10.1902/jop.2015.150223

- 8. Chagas MM, Kobayashi-Velasco S, Gimenez T, Cavalcanti MGP. Diagnostic accuracy of imaging examinations for peri-implant bone defects around titanium and zirconium dioxide implants: A systematic review and meta-analysis. Imaging Sci Dent. 2021;51(4):363-72. https://doi.org/10.5624/isd.20210120
- 9. Varga Jr E, Hammer B, Hardy BM, Kamer L. The accuracy of three-dimensional model generation. What makes it accurate to be used for surgical planning? Int J Oral Maxillofac Surg. 2013;42(9):1159-66.

https://doi.org/10.1016/j.ijom.2013.02.006

- 10. Yousefi F, Shokri A, Zahedi F, Farhadian M. Assessment of the accuracy of laser-scanned models and 3-dimensional rendered cone-beam computed tomographic images compared to digital caliper measurements on plaster casts. Imaging Sci Dent. 2021;51(4):429-38. https://doi.org/10.5624/isd.20210142
- 11. Rangel FA, Maal TJJ, Bronkhorst EM, Breuning KH, Schols JGJH, Bergé SJ, et al. Accuracy and reliability of a novel method for fusion of digital dental casts and cone beam computed tomography scans. PLoS One. 2013;8(3):e59130. https://doi.org/10.1371/journal.pone.0059130
- 12. Flügge T, Derksen W, Poel JT, Hassan B, Nelson K, Wismeijer D. Registration of cone beam computed tomography data and intraoral surface scans A prerequisite for guided implant surgery with CAD/CAM drilling guides. Clin Oral Implants Res. 2017;28(9):1113-18. https://doi.org/10.1111/clr.12925
- 13. Freitas APLF, Peixoto LR, Suassuna FCM, Bento PM, Amorim AMAM, et al. The effects of different metal posts, cements, and exposure parameters on cone-beam computed tomography artifacts. Imaging Sci Dent. 2023;53(2):127-35. https://doi.org/10.5624/isd.20220185
- 14. Schulze R, Heil U, Gross D, Bruellmann DD, Dranischnikow E, Schwanecke U, et al. Artefacts in CBCT: a review. Dentomaxillofac Radiol. 2011;40(5):265-73. https://doi.org/10.1259/dmfr/30642039
- 15. Nkenke E, Zachow S, Benz M, Maier T, Veit K, Kramer M, et al. Fusion of computed tomography data and optical 3D images of the dentition for streak artefact correction in the simulation of orthognathic surgery. Dentomaxillofac Radiol. 2004;33(4):226-32. https://doi.org/10.1259/dmfr/27071199
- 16. Swennen GR, Barth EL, Eulzer C, Schutyser F. The use of a new 3D splint and double CT scan procedure to obtain an accurate anatomic virtual augmented model of the skull. Int J Oral Maxillofac Surg. 2007;36(2):146-52. https://doi.org/10.1016/j.ijom.2006.09.019
- 17. Swennen GR, Mommaerts MY, Abeloos J, De Clercq C, Lamoral P, Neyt N, et al. The use of a wax bite wafer and a double computed tomography scan procedure to obtain a three-dimensional augmented virtual skull model. J Craniofac Surg. 2007;18(3):533-9. https://doi.org/10.1097/scs.0b013e31805343df
- 18. Plooij JM, Maal TJJ, Haers P, Borstlap WA, Kuijpers-Jagtman AM, Bergé SJ. Digital three-dimensional image fusion processes for planning and evaluating orthodontics and orthognathic surgery. A systematic review. Int J Oral Maxillofac Surg. 2011;40(4):341-52. https://doi.org/10.1016/j.ijom.2010.10.013

- 19. Cavalcanti MGP. Cone beam computed tomographic imaging: perspective, challenges, and the impact of near-trend future applications. J Caniofac Surg. 2012;23(1):279-82. https://doi.org/10.1097/SCS.0b013e318241ba64
- 20. Behneke A, Burwinkel M, Behneke N. Factors influencing transfer accuracy of cone beam CT-derived template-based implant placement. Clin Oral Implants Res. 2012;23(4):416-23. https://doi.org/10.1111/j.1600-0501.2011.02337.x
- 21. Queiroz PM, Santaella GM, Paz TDJ, Freitas DQ. Evaluation of a metal artefact reduction tool on different positions of a metal object in the FOV. Dentomaxillofac Radiol. 2017;46(3):20160366.

https://doi.org/10.1259/dmfr.20160366

- 22. Sheikhi M, Behfarnia P, Mostajabi M, Nasri N. The efficacy of metal artifact reduction (MAR) algorithm in cone-beam computed tomography on the diagnostic accuracy of fenestration and dehiscence around dental implants. J Periodontol. 2020;91(2):209-14. https://doi.org/10.1002/JPER.18-0433
- 23. Tahmaseb A, Wu V, Wismeijer D, Coucke W, Evans C. The accuracy of static computer-aided implant surgery: A systematic review and meta-analysis. Clin Oral Implants Res. 2018;29(Suppl 16):416-35.

https://doi.org/10.1111/clr.13346

24. Tahmaseb A, Wismeijer D, Coucke W, Derksen W. Computer technology applications in surgical implant dentistry: a systematic review. Int J Oral Maxillofac Implants. 2014;29(Suppl):25-42.

https://doi.org/10.11607/jomi.2014suppl.g1.2

25. Modica F, Fava C, Benech A, Preti G. Radiologic-prosthetic planning of the surgical phase of the treatment of edentulism by osseointegrated implants: An in vitro study. J Prosthet Dent. 1991;65(4):541-6.

https://doi.org/10.1016/0022-3913(91)90297-a

- 26. Vercruyssen M, Jacobs R, Van Assche N, van Steenberghe D. The use of CT scan-based planning for oral rehabilitation using implants and its transfer to the surgical field: A critical review on accuracy. J. Oral Rehabil. 2008;35(6):454-74. https://doi.org/10.1111/j.1365-2842.2007.01816.x
- 27. Kernen F, Kramer J, Wanner L, Wismeijer D, Nelson K, Flügge T. A review of virtual planning software for guided implant surgery Data import and visualization, drill guide design and manufacturing. BMC Oral Health. 2020;20(1):251. https://doi.org/10.1186/s12903-020-01208-1
- 28. Wismeijer D, Joda T, Flügge T, Fokas G, Tahmaseb A, Bechelli, D, et al. Group 5 ITI Consensus Report: Digital technologies. Clin Oral Implant. Res. 2018;29(Suppl 16):436-42. https://doi.org/10.1111/clr.13309

29. Cattoni F, Chirico L, Merlone A, Manacorda M, Vinci R, Gherlone EF. Digital Smile Designed Computer-Aided Surgery versus Traditional Workflow in "All on Four" Rehabilitations: A Randomized Clinical Trial with 4-Year Follow-Up. Int J Environ Res Public Health 2021;18(7):3449.

https://doi.org/10.3390/ijerph18073449

30. Vahdani N, Moudi E, Ghobadi F, Mohammadi E, Bijani A, Haghanifar S. Evaluation of the Metal Artifact Caused by Dental Implants in Cone Beam Computed Tomography Images. Maedica (Bucur). 2020;15(2):224-9.

https://doi.org/10.26574/maedica.2020.15.2.224

- 31. Machado AH, Fardim KAC, Souza CF, Sotto-Maior BS, Assis NMSP, Devito KL. Effect of anatomical region on the formation of metal artefacts produced by dental implants in cone beam computed tomographic images. Dentomaxillofac Radiol. 2018;47(3):20170281. https://doi.org/10.1259/dmfr.20170281
- 32. Cebe F, Aktan AM, Ozsevik AS, Ciftci ME, Surmelioglu HD. The effects of different restorative materials on the detection of approximal caries in cone-beam computed tomography scans with and without metal artifact reduction mode. Oral Surg Oral Med Oral Pathol Oral Radiol. 2017;123(3):392-400.

https://doi.org/10.1016/j.oooo.2016.11.008

33. Alaidrous M, Finkelman M, Kudara Y, Campos HC, Kim Y, Souza AB. Influence of zirconia crown artifacts on cone beam computed tomography scans and image superimposition of tomographic image and tooth surface scan: An in vitro study. J Prosthet Dent. 2021;125(4):684.e1-684.e8.

https://doi.org/10.1016/j.prosdent.2020.06.028

34. Kocasarac H, Koenig LJ, Ustaoglu G, Oliveira ML, Freitas DQ. CBCT image artefacts generated by implants located inside the field of view or in the exomass. Dentomaxillofac Radiol. 2022;51(2):20210092.

https://doi.org/10.1259/dmfr.20210092

- 35. Hinchy NV, Anderson NK, Mahdian M. Metal artifact reduction using common dental materials. Dentomaxillofac Radiol 2022:51(2):20210302. https://doi.org/10.1259/dmfr.20210302
- 36. Fontenele RC, Nascimento EH, Vasconcelos TV, Noujeim M, Freitas DQ. Magnitude of cone beam CT image artifacts related to zirconium and titanium implants: impact on image quality. Dentomaxillofac Radiol. 2018;47(6):20180021. https://doi.org/10.1259/dmfr.20180021

Figure 1: Superimposition of the corresponding STL file based on four fixed anatomical positions on the 3D arches. These landmarks were defined as: a) Vertical/Posterior (VP): Selecting a posterior tooth and measuring the distance between the STL file and the occlusal surface of the tooth (tip of the canine). b) Horizontal/Posterior (HP): After selecting a posterior tooth, the distance between the STL file and the buccal surface was measured. c) Vertical/Anterior (VA): Selecting an anterior tooth and measuring the distance between the STL file and the incisal surface of the tooth. d) Horizontal/Anterior (HA): After selecting an anterior tooth, the distance between the STL file and the buccal surface was measured.

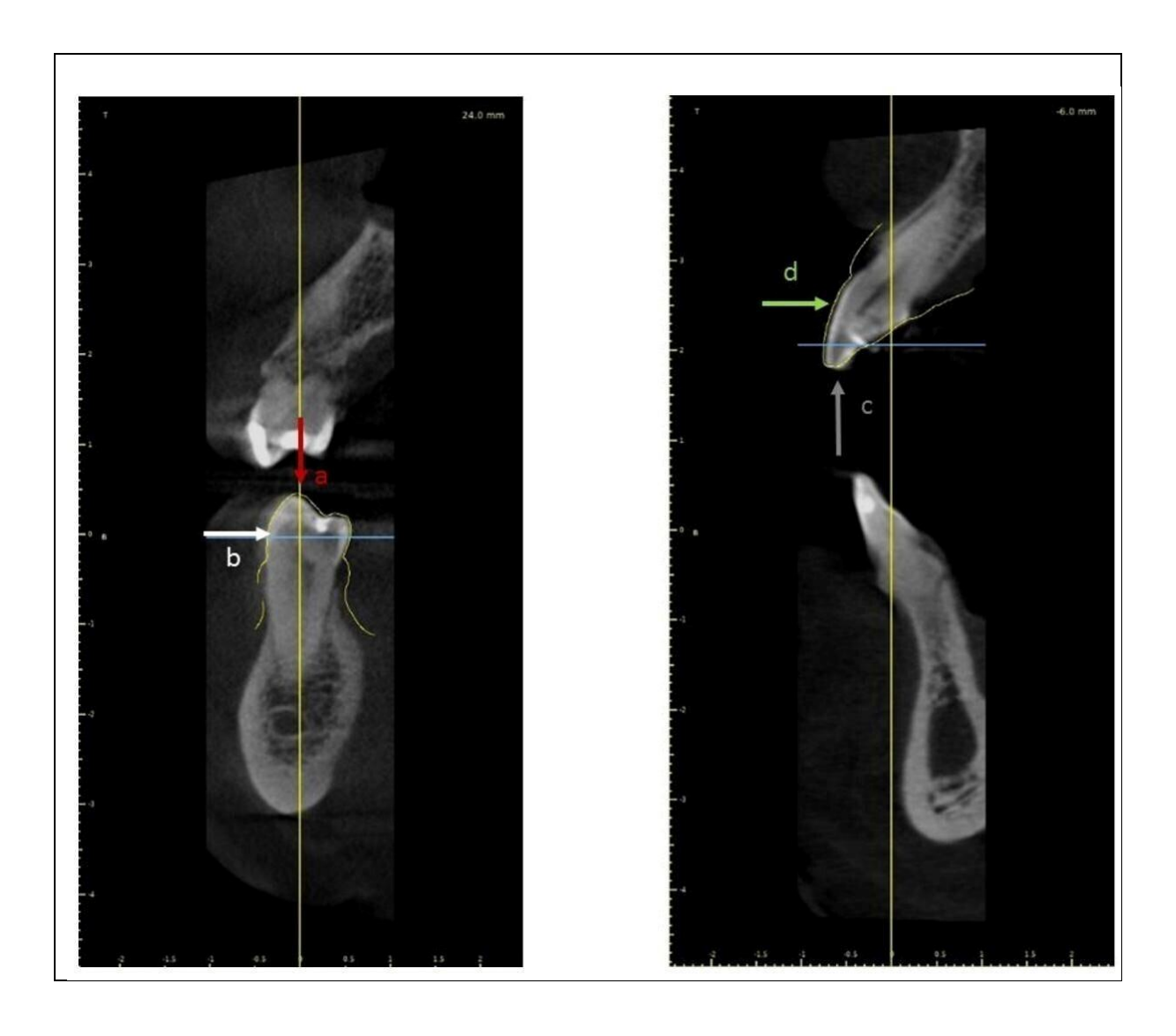


Figure 2: On the left, coronal section of the molar region; On the right, sagittal section of the central incisor region, denoting the failure in the overlapping of the systems, demarcated and signaled by the green contour, obtained by the Image J software.

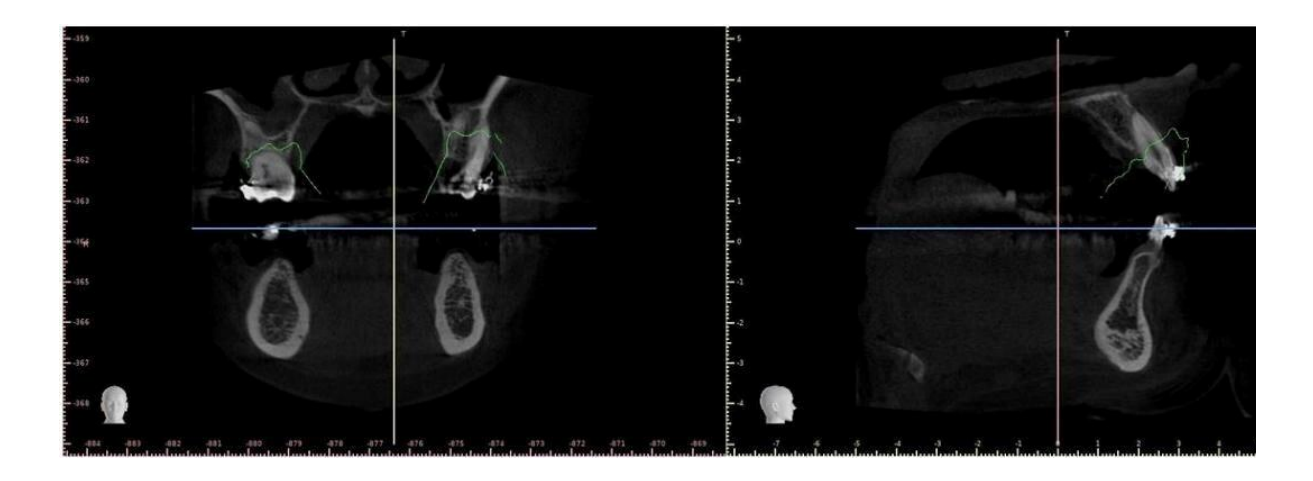


Table 1: Positions determined concerning the number of metallic restorations.

Positions	Groups*	N	Mean	Standard Deviation	Median	First quartile	Third quartile	p**
Vertical_posterior (VP)	0	18	0.4049	±1.068	0.0465	0.0215	0.1265	0.738
	1	19	0.4629	± 0.754	0.18	0.034	0.541	
	2	32	0.6132	± 1.002	0.0395	0.0238	0.7275	
	0	16	0.088	± 0.111	0.052	0.0248	0.0845	0.141
Horizontal_posterior	1	18	0.314	± 0.547	0.104	0.0163	0.3283	
(HP)	2	24	0.1472	± 0.489	0.021	0.0075	0.0725	
	0	18	0.7888	±1.329	0.0365	0.018	0.8665	0.555
Vertical_anterior	1	22	0.9727	± 1.353	0.2465	0.0388	1.3825	
(VA)	2	34	0.8384	± 1.128	0.0495	0.013	1.3263	
Horizontal anterior (HA)	0	15	0.1056	± 0.237	0.0165	0.0108	0.0465	***0.009
	1	19	0.3071	± 0.385	0.0935	0.0275	0.419	
•	2	22	0.0628	± 0.110	0.019	0.0025	0.0485	

^{*} Group 0: 0-2 metallic restorations; Group 1: 3-5 metallic restorations; Group 2: 6 or more metallic restorations; **Kruskal-Wallis test; ***p≤0.05 (statistically significant difference).

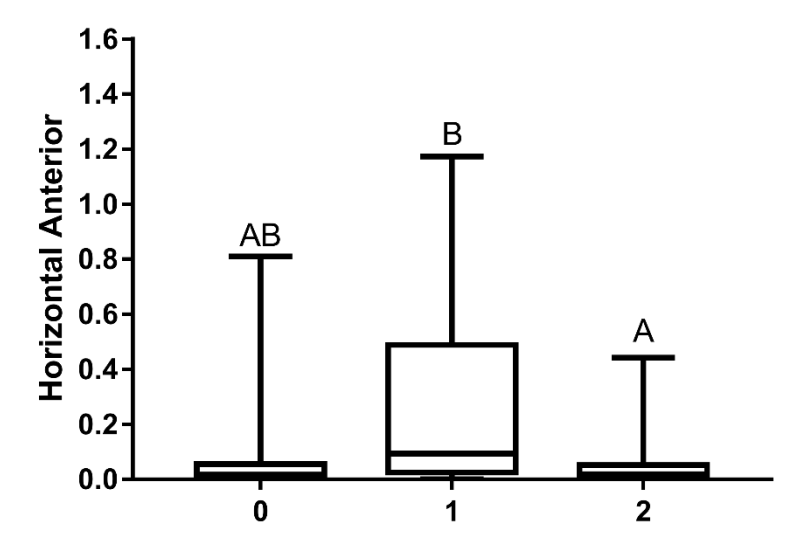


Figure 3: Boxplot showing median, maximum, and minimum, with the application of the Kruskal-Wallis test and post-Dunn's test.

Table 2: Comparison of the occlusion and non-occlusion during the acquisition, with the mean, standard deviation, median, quartiles, and p-value, applying the for independent variables.

Positions	Groups*	N	Mean	Standard Deviation	Median	First quartile	Third quartile	p**
Vertical_posterior (VP)	0	41	0.311	±0.713	0.46	0.036	0.954	***0.029
	1	28	0.82	±1.165	0.031	0.019	0.117	
Horizontal_posterior	0	38	0.183	±0.534	0.1385	0.0188	0.3188	0.978
(HP)	1	20	0.181	±0.195	0.033	0.0129	0.0665	
Vertical_anterior	0	48	0.717	±1.228	0.0418	1.7585	1.7168	***0.006
(VA)	1	26	1.143	±1.216	0.0125	0.9625	0.95	
Horizontal_anterior (HA)	0	37	0.101	±0.209	0.068	0.012	0.451	0.204
	1	19	0.266	±0.369	0.024	0.0113	0.0528	·•

^{*}Group 0: closed mouth; Group 1: open mouth; ** Mann-Whitney Test; ***p≤0.05 (statistically significant difference).

Table 3: Occlusion pattern, applying the Mann-Whitney Test for independent variables.

Positions	Groups*	N	Mean	Standard Deviation	Median	First quartile	Third quartile	p**
Vertical posterior (VP)	0	41	0.3394	±0.713	0.039	0.0185	0.45	
	1	28	0.8978	±1.165	0.061	0.0335	1.5125	***0.004
Horizontal_posterior	0	38	0.1754	±0.534	0.04	0.0085	0.224	0.101
(HP)	1	20	0.2034	±0.195	0.034	0.0185	0.0875	
Vertical_anterior	0	48	0.4736	±1.228	0.0375	0.0138	0.7988	
(VA)	1	26	1.4422	±1.216	0.9285	0.029	3.0873	***0.016
Horizontal_anterior (HÁ)	0	37	0.2031	±0.209	0.036	0.011	0.296	0.284
	1	19	0.0295	±0.369	0.0185	0.0125	0.0393	0.204

^{*}Group 0: Upper arch (maxillary); Group 1: Lower arch (jaw); **Mann-Whitney Test; ***p≤0.05 (statistically significant difference).